The impact of temperature errors on perceived humidity supersaturation

S. A. Buehler and N. Courcoux

Institute of Environmental Physics, University of Bremen, Bremen, Germany

Received 6 May 2003; revised 6 June 2003; accepted 17 June 2003; published 25 July 2003.

[1] A Monte Carlo method is used to study the propagation of temperature uncertainties into relative humidity with respect to ice (RH_i) calculated from specific humidity. For a flat specific humidity distribution and Gaussian temperature uncertainties the resulting RH_i distribution drops exponentially at high RH_i values—much slower than a Gaussian. This agrees well with the RH_i distribution measured by the Microwave Limb Sounder (MLS), which means that such remotely measured RH_i distributions can be explained, at least partly, by temperature uncertainties. *INDEX TERMS:* 1640 Global Change: Remote sensing; 1655 Global Change: Water cycles (1836); 1694 Global Change: Instruments and techniques; 3399 Meteorology and Atmospheric Dynamics: General or miscellaneous. **Citation:** Buehler, S., and N. Courcoux, The impact of temperature errors on perceived humidity supersaturation, *Geophys. Res. Lett.*, *30*(14), 1759, doi:10.1029/2003GL017691, 2003.

1. Introduction

[2] The equilibrium vapor pressure of water molecules over a plane surface of liquid water (e_w) or ice (e_i) depends only on temperature (T) (Strictly, this is only true for water vapor in the pure phase. If water vapor is mixed in air, e_w and e_i are slightly enhanced. However, the enhancement is below 0.5% according to *Sonntag* [1994], and hence can be safely neglected for the purpose of this paper.) There are a number of empirical formulas in use to calculate $e_w(T)$ and $e_i(T)$. The calculations presented here are based on the formulas by *Sonntag* [1994], but differences between the different parameterizations are small and have no impact on the results. Figure 1 shows $e_w(T)$ and $e_i(T)$. The curves separate at $T = 0°C$, at higher temperature $e_i(T)$ is not defined. Note the strong and non-linear temperature dependence.

[3] The equilibrium water vapor pressure is used to define relative humidity with respect to liquid water (RH_w) and ice (RH_i):

$$RH_w = \frac{e}{e_w(T)} \qquad RH_i = \frac{e}{e_i(T)} \tag{1}$$

where e is the actual water vapor pressure. Because e_i is lower than e_w, RH_i will always be higher than RH_w. Thus, it is possible that RH_i exceeds 100%, while RH_w is still below 100%.

[4] While $RH_w > 100\%$ does not occur in the Earth's atmosphere, $RH_i > 100\%$ does occur quite frequently, as is well documented for example by *Wallace and Hobbs* [1977]. The phenomenon can be explained with the absence of ice nuclei. Such supersaturation with respect to ice recently has received a lot of attention [*Spichtinger et al.* [2002b], *Gierens et al.* [1999], *Jensen et al.* [2001]]. As an example, Figure 2 shows a distribution of RH_i at 215 hPa derived from the UARS MLS UTH data set, which has been described by *Read et al.* [2001]. This figure is roughly the same as Figure 1 in *Spichtinger et al.* [2002b].

[5] A closer inspection of Figure 2 reveals that some of the data points show even supersaturation with respect to liquid water. Consider the ratio of $e_w(T)/e_i(T)$, which is displayed in Figure 3. At a temperature of 220 K, consistent with the chosen altitude, the ratio is approximately 1.7, which means that RH_i values above 170% are above liquid water saturation and hence rather unlikely. It should be noted that *Read et al.* [2001] themselves recommend to set data above 120% RH_i to 100%, for completely different reasons related to the radiative effect of cirrus clouds.

[6] Ignoring these problems and using the data anyway for arguments sake, one can say that the problem with the distribution shown in Figure 2 is that all remote sensing methods rely on the fundamental law stating that the amount of radiation absorbed, emitted, or scattered is proportional to the amount of the interacting substance. (For extinction, this is stated by the Lambert-Beer law.) Hence, any remote sensing method will not measure relative humidity, but absolute humidity. An absolute humidity parameter is for example the specific humidity (q), defined as

$$q = \frac{m_w}{m_w + m_a} \qquad \left[\frac{kg}{kg}\right] \tag{2}$$

where m_w is the mass of water molecules in a unit volume, and m_a is the mass of other air molecules.

[7] To convert from q to RH_i, one must know the equilibrium water vapor pressure $e_i(T)$, hence the temperature T. However, T will generally be known only with a limited accuracy. The purpose of this study is to demonstrate how uncertainties in T will lead to apparent supersaturation, even if there is no true supersaturation.

2. Methodology

[8] A Monte Carlo approach was chosen for the study. This has the advantage that non-Gaussian statistics and nonlinearities can be correctly taken into account. As a simplistic example, assume that the true RH_i is 100%. Assuming fixed temperature T and pressure p, this can be converted to a q value. The T uncertainty is modeled by creating a random ensemble of $T^{(j)}$ values representing a Gaussian distribution around the correct T (Figure 4, plot a). The index j runs from 1 to the total number of values in the ensemble (N), in this

0094-8276/03/2003GL017691$05.00

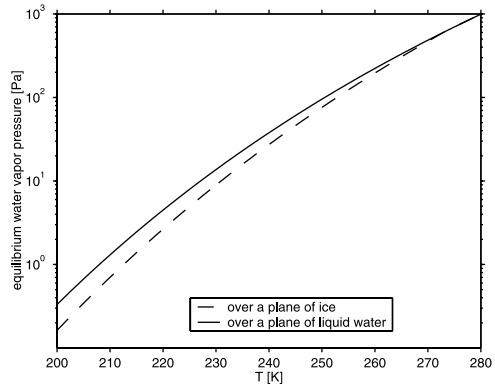

Figure 1. Equilibrium water vapor pressure over liquid water (solid line) and over ice (dashed line) as a function of temperature. Note the logarithmic scale.

case $N = 10^7$. The ensemble size N just has to be large enough to obtain a smooth distribution. A Gaussian distribution was chosen because in the absence of other information this can be taken as representative for typical measurement errors.

[9] The temperature ensemble can be used to simulate an ensemble

$$\mathrm{RH}_i^{(j)} = \frac{e(q)}{e_i(T^{(j)})} \tag{3}$$

of measured RH_i values (Figure 4, plot b). Note that the distribution of the $\mathrm{RH}_i^{(j)}$ ensemble is not Gaussian, but has a much higher tail towards high RH_i values.

[10] In contrast, Gaussian errors on the measurement of q will lead to also Gaussian errors on the RH_i, as demonstrated by Figure 4, plots c and d.

3. Setup

[11] A very simple setup was chosen for the study, because the aim is to illustrate a fundamental point, not to be as realistic as possible. Pressure and true temperature are assumed to be fixed at $p = 215$ hPa and $T = 220$ K, consistent with average midlatitude upper troposphere conditions. This is the same pressure level that was used in *Spichtinger et al.* [2002b]. For these conditions $\mathrm{RH}_i = 100\%$ corresponds to $q = 7.6742 \times 10^{-5}$ kg/kg.

[12] The true RH_i distribution was assumed to be flat for $\mathrm{RH}_i \leq 100\%$ and zero for $\mathrm{RH}_i > 100$. (All RH_i values below 100% are equally likely.) Although a flat distribution is a rather simplistic assumption, it is well supported by radiosonde data, as shown in Figure 5. The sharp cut at $\mathrm{RH}_i = 100\%$ is for arguments sake only, in reality there will be some supersaturation.

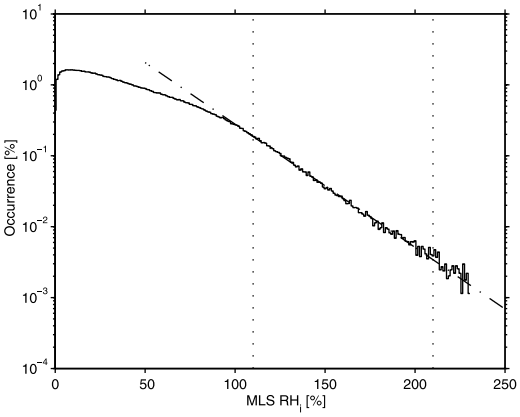

Figure 2. Distribution (fractional occurrence per 1% RH_i bin) of relative humidity with respect to ice (RH_i) at 215 hPa, derived from the UARS MLS UTH data set (solid line). A fitted exponential function (dashed-dotted line) shows that the number of occurrences decreases exponentially with increasing RH_i between 100% and 230%. Vertical dotted lines indicate fitting boundaries. See Table 1 for the parameters of the fitted line.

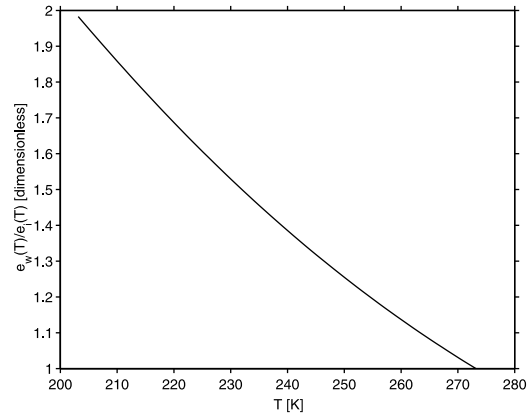

Figure 3. Ratio of equilibrium water vapor pressure over a plane of liquid water ($e_w(T)$) and equilibrium water vapor pressure over a plane of ice ($e_i(T)$) plotted against temperature (T).

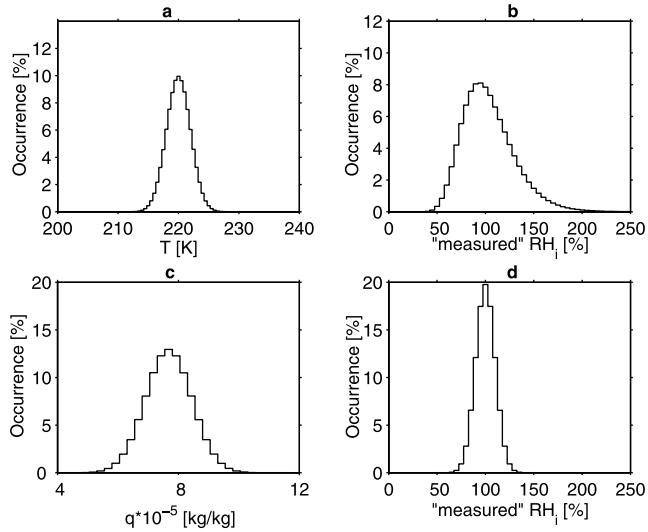

Figure 4. Top: Mapping of temperature uncertainties. Shown are distributions of temperature measurement error (a) and the resulting "measured" relative humidity with respect to ice (b). Bottom: Mapping of humidity uncertainties. Shown are distributions of specific humidity measurement error (c) and again the resulting "measured" relative humidity with respect to ice (d). Note that only temperature errors lead to an asymmetric relative humidity distribution.

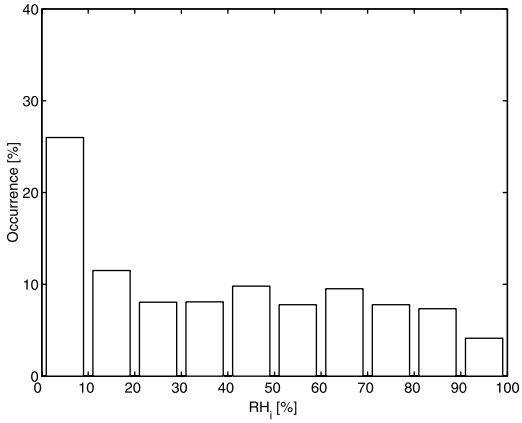

Figure 5. The distribution of relative humidity with respect to ice at 215 hPa from Lindenberg radiosonde data ([*Leiterer et al.*, 1997]), for the time period January to December 2001. As described by *Leiterer et al.*, [1997], particular care has been taken to correct and quality-control these data for the low humidities and cold temperatures typical for the upper troposphere.

[13] The temperature measurement error was assumed to follow a Gaussian distribution with a standard deviation of initially $\sigma_T = 2$ K, a typical value that was also assumed by *Read et al.* [2001] The measurement error in q is assumed to be $\sigma_q = 7.6742 \times 10^{-6}$ kg/kg = 10%.

4. Results and Discussion

[14] Figure 6 shows the simulated measured RH_i separately for (a) only 2 K temperature error and (b) only 10% specific humidity error. The distribution (a) is very similar to the one found for the MLS data (compare Figure 2). In particular, it drops off much slower at high supersaturation

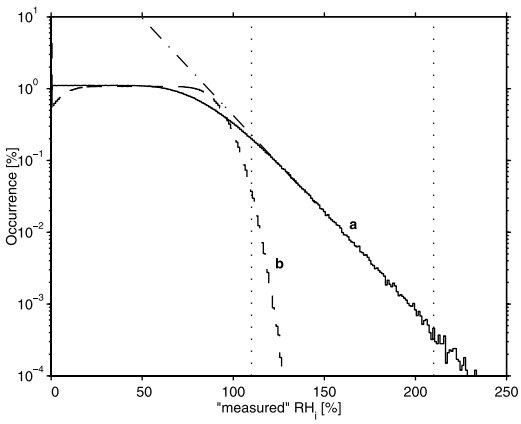

Figure 6. Distributions (occurrence per 1% RH_i bin) of "measured" relative humidity with respect to ice computed from specific humidity. Solid line (a): considering only temperature measurement errors, dashed line (b): considering only specific humidity measurement errors. As in Figure 2 the fitted straight line shows that the number of occurrences decreases exponentially with increasing RH_i for curve (a). Vertical dotted lines show fitting boundaries. See Table 1 for the actual fit parameters.

Table 1. Relative Humidity Standard Deviations (σ_{RH_i}) and Fitted Exponents B for the Exponential Drop-Off of the $p(S)$ Distribution for Different Temperature Uncertainties

Case	σ_{RH_i} (lin)	σ_{RH_i} (MC)	B * 100	Fitted Range
$\sigma_T = 0.5$ K	6.4%	6.4%	36.9	100–115% RH_i
SP Lind.			21	
$\sigma_T = 1$ K	12.7%	12.9%	17.3	110–145% RH_i
$\sigma_T = 2$ K	25.4%	26.9%	6.3	110–210% RH_i
SP MLS			4.6	
MLS			4.0	
$\sigma_T = 2.7$ K	34.3%	38.2%	4.0	110–210% RH_i
$\sigma_T = 3$ K	38.1%	43.6%	3.5	110–210% RH_i
$\sigma_T = 5$ K	63.5%	93.5%	1.9	110–210% RH_i

The σ_{RH_i} have been calculated in two different ways, by linear error propagation ("lin") using dRH_i/dT, and by our Monte Carlo method ("MC"). The value marked "SP Lind." is found by *Spichtinger et al.* [2002a] for Lindenberg radiosonde data, the value marked "SP MLS" is found by *Spichtinger et al.* [2002b] for global tropospheric MLS data. The value marked "MLS" is the one from our own fit to MLS data presented in Figure 2. The last column indicates the RH_i range that was used to determine B. For smaller σ_T values this has to be closer to 100%, since the drop-off is faster.

values than a Gaussian distribution. The drop-off behavior can be well described by a simple exponential function.

[15] Such a distribution cannot be explained by specific humidity measurement errors, as should be clear from curve (b). In fact, to obtain the observed probability of 9×10^{-6} at 200% RH_i, one would have to assume a σ_q of 36%, a value that is unrealistically high. Furthermore, the distribution would not have the same exponential drop-off behavior.

[16] An exponential function of the form

$$p(S) = A\, e^{-BS} \tag{4}$$

was fitted to both MLS data and Monte Carlo results. Here, $S = RH_i - 100\%$ is the supersaturation, $p(S)$ is the probability to find supersaturation value S, and A and B are fit parameters. The results are summarized in Table 1.

[17] The table can also be used to estimate what accuracy of temperature knowledge would be necessary to do supersaturation studies with remote sensing data. Of course, if the statistics of the temperature errors were known exactly, their impact could be removed by calculations similar to those

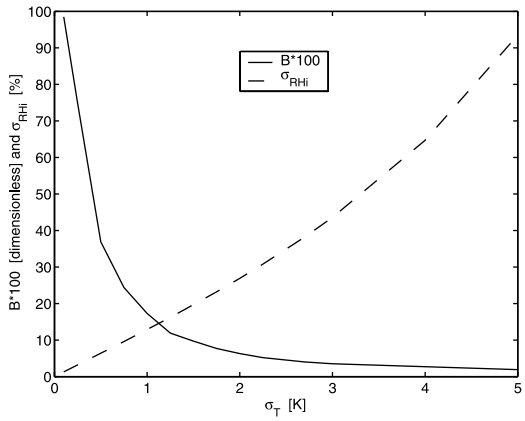

Figure 7. Fitted exponent for the exponential drop-off of the $p(S)$ distribution (B) and relative humidity standard deviation (σ_{RH_i}) as a function of temperature standard deviation (σ_T).

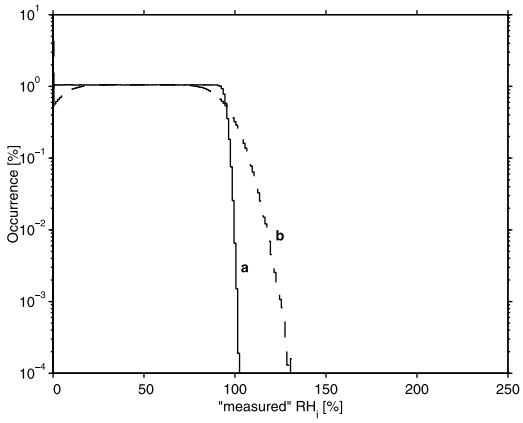

Figure 8. Distributions of "measured" relative humidity with respect to ice (RH_i) computed from relative humidity with respect to liquid water (RH_w). Solid line (a): considering only T measurement errors, dashed line (b): considering only RH_w measurement errors.

presented in this paper, so that the magnitude of the σ_T would not matter. However, it is unlikely that the statistics will be sufficiently well known for real data. A conservative approach is to demand that the drop-off resulting from the temperature uncertainty should be significantly steeper than the one resulting from true supersaturation. As observed drop-off coefficients B are as large as 0.21 [*Spichtinger et al.*, 2002a], σ_T would have to be around 0.5 K or smaller.

[18] Figure 7 shows the B parameter as a function of σ_T. It can be used to infer the necessary temperature precision, if one wants to detect supersaturation with a certain drop-off characteristic. Standard deviations of RH_i are also shown. For example, a σ_T of 2 K would result in a σ_{RH_i} of 27%. This value is compatible to the error analysis of *Read et al.* [2001], who also assumed 2 K for σ_T and estimate the total σ_{RH_i} as 10–30% depending on height and latitude bin (this includes also other error sources, not just temperature). Our value being in the upper part of this range is partially due to the fact that the Monte Carlo method takes into account the nonlinearity. Simple linear error propagation (shown also in Table 1 for comparison) leads to somewhat lower values, but for $\sigma_T = 2$ K this effect is still small. The more important reason is that the σ_{RH_i} value scales with the actual value of RH_i and we have assumed the true RH_i to be 100%. Thus, for drier conditions the σ_{RH_i} value is much smaller.

[19] In a final step, it was also investigated how temperature errors influence the result if RH_w is measured and RH_i is calculated from that. This is the normal case if radiosonde data from Vaisala humidity sensors are used. The results are shown in Figure 8, again separately for a 2 K temperature error and a 10% error in RH_w. The figure shows that in this case temperature errors are not critical. This can be explained with the fact that while $e_i(T)$ and $e_w(T)$ are strongly nonlinear functions, the ratio $e_w(T)/e_i(T)$ is a close to linear function (Figure 3). It should be noted, though, that radiosondes may have other problems at high humidities and cold temperatures, such as icing, which are not discussed here.

5. Conclusions

[20] Temperature uncertainties have a strong impact on perceived supersaturation if the relative humidity is calculated from measurements of absolute humidity. Even for moderate temperature uncertainties, very high perceived supersaturation can occur, because the strongly non-linear temperature dependence of the equilibrium water vapor pressure enhances the 'tail' of the distribution towards high RH values. The resulting distribution for a flat q distribution and a Gaussian T error distribution is non-Gaussian, featuring an exponential drop-off behavior towards high RH values.

[21] With an assumed T uncertainty of 2.7 K, the RH_i distribution measured by MLS can be reproduced without assuming any 'real' supersaturation. However, the point of this study is not to deny the reality of supersaturation, but to emphasize that the use of remotely sensed data for studies of supersaturation is problematic, and in particular requires a careful analysis of the influence of temperature uncertainties. A T uncertainty of 2 K, as assumed in *Read et al.* [2001], would still account for a large part of the observed supersaturation.

[22] **Acknowledgments.** We thank Peter Spichtinger, DLR, for a discussion that lead to the idea of this paper. We also thank Ulrich Leiterer and Horst Dier from DWD station Lindenberg for fruitful discussions and radiosonde data. We thank the MLS team, in particular W. Read, and the NASA GSFC Earth Sciences Distributed Active Archive Center (DAAC) for MLS data and explanations. Furthermore, we thank Mashrabjon Kuvatov for obtaining, extracting, and analyzing the MLS data. Last but not least, we thank the two reviewers for their constructive and helpful comments.

[23] This study was funded by the German Federal Ministry of Education and Research (BMBF), within the AFO2000 project UTH-MOS, grant 07ATC04. It is a contribution to COST Action 723 'Data Exploitation and Modeling for the Upper Troposphere and Lower Stratosphere'.

References

Gierens, K., U. Schumann, M. Helten, H. Smit, and A. Marenco, A distribution law for relative humidity in the upper troposphere and lower stratosphere derived from three years of MOZAIC measurements, *Ann. Geophys.*, *17*, 1218–1226, 1999.

Jensen, E. J., et al., Prevalence of ice-supersaturated regions in the upper troposphere: Implications for optically thin cloud formation, *J. Geophys. Res.*, *106*, No.(D15), 17,253–17,266, 2001.

Leiterer, U., H. Dier, and T. Naebert, Improvements in radiosonde humidity profiles using RS80/RS90 radiosondes of Vaisala, *Beitr. Phys. Atmosph.*, *70*, No.(4), 319–336, 1997.

Read, W., et al., UARS microwave limb sounder upper tropospheric humidity measurement: Method and validation, *J. Geophys. Res.*, *106*, No.(D23), 32,207–32,258, 2001.

Sonntag, D., Advancements in the field of hygrometry, *Meteorol. Z.*, *3*, 51–66, 1994.

Spichtinger, P., K. Gierens, U. Leiterer, and H. Dier, Ice supersaturated regions over the station Lindenberg, Institut fuer Physik der Atmosphaere, Report No. 169, DLR - Oberpfaffenhofen, D-82234 Wessling, Germany, 2002a, also in press at Meteorol. Z.

Spichtinger, P., K. Gierens, and W. Read, The statistical distribution law of relative humidity in the global tropopause region, *Meteorol. Z.*, *11*, 83–88, 2002b.

Wallace, J. and P. Hobbs, *Atmospheric science, an introductory survey*, Academic Press, 1977.

S. A. Buehler and N. Courcoux, Institute of Environmental Physics, University of Bremen, Otto-Hahn-Allee 1, D-28259 Bremen, Germany. (sbuehler@uni-bremen.de)